The structural impact of water sorption on device-quality melanin thin films

Andrew J. Clulow[1*], A. Bernardus Mostert[1*], Margarita Sheliakina[1], Andrew Nelson[2], Norman Booth[2], Paul L. Burn[1], Ian R. Gentle[1] and Paul Meredith[3]

[1]*Centre for Organic Photonics & Electronics, The University of Queensland, St Lucia, QLD 4072, Australia*

[2]*Australian Centre for Neutron Scattering, Australian Nuclear Science and Technology Organisation, Locked Bag 2001, Kirrawee DC, NSW 2232, Australia*

[3]*Department of Physics, Swansea University, Singleton Park, SA2 8PP, Wales, United Kingdom*

* andrew.clulow@monash.edu; a.mostert@uq.edu.au

Keywords: Melanin, neutron reflectometry, water sorption, deuteration, thin film structure.

Abstract

The melanins are a class of pigmentary bio-macromolecules ubiquitous in the biosphere. They possess an intriguing set of physico-chemical properties and have in particular been shown to exhibit hybrid protonic-electronic electrical conductivity, a feature derived from a process termed chemical self-doping driven by the sorption of water. Although the mechanism underlying the electrical conduction has been established, how the sorbed water interacts with the melanin structure at the physical level has not. Herein we use neutron reflectometry to study changes in the structure of synthetic melanin thin films as a function of H_2O and D_2O vapour pressure. Water is found to be taken up evenly throughout the films, and by employing the contrast effect, the existence of labile protons through reversible deuterium exchange is demonstrated. Finally, we determine a sorption isotherm to enable quantification of the melanin-water interactions.

Footnotes

Electronic Supplementary Information is available with this article.

Dr Andrew Clulow (current address: Drug Delivery, Disposition and Dynamics, Monash Institute of Pharmaceutical Science, 381 Royal Parade, Parkville, VIC 3052, Australia; email: andrew.clulow@monash.edu) and Dr Bernardus Mostert (current address: Centre for Organic Photonics & Electronics, The University of Queensland, St Lucia, QLD 4072, Australia; email: a.mostert@uq.edu.au) are co-corresponding authors for this article.

Introduction

Eumelanin is a brown-black pigment[1] found in nature and is best known as a photo-protectant against UV radiation[2, 3] in human skin[1]. It is also found in other parts of the body, including the *substantia nigra* of the brain stem[4] (combined with pheomelanin to form neuromelanin[5]) where the exact biological role is still somewhat uncertain. Eumelanin, commonly referred to as simply melanin – the nomenclature to be adopted in this paper, is chemically amorphous being composed of aggregated oligomeric and polymeric species derived from the indolic monomers 5,6-dihydroxyindole (DHI) and 5,6-dihydroxyindole-2-carboxylic acid (DHICA) and their various redox forms[1, 2]. The monomers are randomly cross-linked to form planar sheets that are stacked via aromatic π-interactions and have varying conjugation lengths, disorder and dimensions [6, 7].

Melanin has long interested the materials community because of its novel physico-chemical properties that include: broad-band optical absorption[2, 8, 9]; the presence of persistent free radicals[2, 10-15]; robustness towards exposure to harmful radiation[16]; almost complete non-radiative conversion of absorbed photon energy[8, 17, 18]; and electrical and photo-conductivity[13, 19-23]. The electrical properties are strongly dependent upon the degree of hydration, which has led to the view that the material is a hybrid ionic-electronic conductor[13]. The origin of this hybrid behaviour is a redox reaction, the so-called comproportionation equilibrium (Scheme 1), which yields a chemical self-doping effect whereby one-electron oxidation of the hydro-quinone to the semi-quinone releases protons into the hydrating water matrix. These protons diffuse or drift under the action of an external electric field *via* a Grotthuss Mechanism.[24] Several studies have confirmed this ionic behaviour[20, 22] and a melanin-based battery utilizing the comproportionation principle has been reported.[25]

Due to dual ionic/electronic properties and biocompatibility, melanin is considered a prime candidate material for bioelectronic applications. One of the key challenges in bioelectronics is to interface biological entities with read/write or control electronics.[26-28] Signals in biology invariably originate from the movement of ions, whilst current in conventional semiconductors is carried by electrons and holes. Hence, connecting 'ionics' and electronics requires a biocompatible interface capable of transducing these two electrical phenomena.

Since melanin [and associated poly(indole)s] can be made into device quality thin films[22, 29-34] that retain protonic conduction, the material has the potential to be a model transducing element for bioelectronic applications, especially when used in combination with organic semiconductors. Neat and composite device-quality melanin thin films have been investigated in a variety of applications including transistors, batteries [22, 32, 34], and multifunctional coatings[29, 30]. However, there is currently no direct structural information on how these films interact with a wet environment with

only inferences based on their electrical properties being made.[22, 23, 31, 32] Since hydration is a first order variable on the electrical properties of melanin[13, 19], it is clearly important to understand the structural consequences of hydration. Gravimetric adsorption isotherms for melanin exposed to H_2O and D_2O vapour have been reported for pressed powder pellets of melanin[15, 35], but there are no such reports for melanin thin films. Furthermore, it would be useful to gain information on how the water is distributed throughout a film since this impacts performance parameters such as responsivity, speed, stability, and reproducibility.

Neutron reflectometry (NR) is a means to directly and non-invasively study thin film structure and particularly how it evolves as a function of time, temperature, and other environmental factors such as hydration. In an NR experiment, neutrons are directed onto a thin film sample and are reflected to some degree by each stratum. The reflected waves from each stratus interfere with one-another, leading to fringes in the reflectivity as a function of momentum transfer, $Q = \frac{4\pi \sin\theta}{\lambda}$ where θ is the angle of incidence and λ is the neutron wavelength. The spacing between the fringes is directly related to the thickness of layers within the sample and their amplitude is governed by the Scattering Length Density [SLD, Equation (1)] of the layers. The SLD is the product of the sum of the bound coherent neutron scattering lengths of the constituent atoms in a molecule and the number density of said molecules within the film. When films are exposed to H_2O and D_2O vapour the contrast in neutron scattering lengths of hydrogen (b_H = -3.74 fm) and deuterium (b_D = 6.67 fm) nuclei means that the films scatter quite differently when there is solvent penetration, and/or proton exchange, because the overall SLD of the film changes markedly.[36] The sorption of water into melanin and the corresponding structural changes can then be modelled as changes in film SLD as a function of distance from the substrate by least squares analysis of the observed reflectivity profiles.[37]

Herein, we present a NR experiment on melanin thin films exposed to water vapour at systematically varying pressures with the neutron reflectivity profiles recorded *in situ*. The experimental setup involves a vacuum line with an automated static vapour delivery system. Samples were exposed to the same relative humidities of H_2O and D_2O, and the chamber was evacuated between exposures to observe the reversibility of the hydration process. The static (not kinetic) delivery system enables a thermodynamic equilibrium to be achieved[38] and controls the absolute pressure of the water vapour admitted to the sample chamber. This method overcomes the errors associated with using saturated salt solutions, where it is generally assumed that the same salt yields the same relative humidity for both H_2O and D_2O.[39] However, this assumption is not correct as the saturated vapour pressures of H_2O and D_2O differ by around 20% at ambient conditions.[40, 41]

Experimental Methods

Melanin synthesis and thin film preparation: Melanin was synthesised following a standard literature procedure,[11, 35] utilizing as the initial starting material D,L-dopa (Sigma-Aldrich). In brief, the D,L-dopa was dissolved in deionised water, subsequently adjusted to pH 8 using NH_3 (aq., 28%). Air was then bubbled through the solution under stirring for 3 days. The solution was then brought to pH 2 using HCl (aq., 32%) to precipitate the pigment. The solution was then filtered and washed multiple times with deionised water and dried. The resulting powder was then suspended in an ammonia solution as described in previously published work,[33] for spin-coating. Briefly, the solution composition was ~0.7 g melanin in 5 mL H_2O and 10 mL NH_3 (aq., 28%), which was stirred for 1 hour at room temperature and the ultrasonicated for 1 hour. Two different sets of substrates were prepared. The NR and X-ray reflectometry (XRR) studies were prepared on silicon wafers of 50 mm diameter, which were initially cleaned in Piranha solution [a mixture of sulfuric acid (98%, 245 mL) and hydrogen peroxide (30%, 105 mL)], followed by a UV-Ozone (20 min) treatment. The second set of substrates for X-ray photoelectron spectroscopy (XPS) studies were 15 mm x 15 mm silicon wafers, which were cleaned with a warm soap solution (Alcanox), rinsed in water and ultra-sonicated in acetone (5 min). These latter substrates were then rinsed with deionised water, ultra-sonicated in 2-propanol (5 min) and dried under a flow of nitrogen. The substrates were then finally treated with UV-Ozone (20 min). Melanin films were then deposited on the cleaned wafers in air by spin-coating at 1500 rpm for 60 s from the solution described above. Films for the NR, XRR and XPS experiments were prepared at the same time from the same melanin solution.

Neutron Reflectometry measurements: The measurements were performed using the *PLATYPUS* time-of-flight neutron reflectometer operating in medium resolution mode, ($\Delta Q/Q$ = 4.5%) with a cold neutron spectrum (2.8 Å < λ < 18.0 Å) at the OPAL 20 MW research reactor [Australian Nuclear Science and Technology Organisation (ANSTO), Sydney, Australia].[42] The samples were placed on top of a boron carbide block in a sealed sample chamber custom built for use on *PLATYPUS*. The chamber is connected to a computer controlled ANSTO "static" vapour pressure system supplied by Hiden Isochema to an original design based on their XCS sample climate control system. The vapour pressure above the sample was controlled by two needle valves; one connected to a turbo pump and the other to a heated liquid reservoir that contained either H_2O or D_2O in these experiments. The sample chamber was equilibrated to 25 ºC, while the sample climate control system and vapour transfer lines were equilibrated to 50 ºC to prevent condensation within the delivery system. H_2O and D_2O were initially degassed with four freeze-pump-thaw cycles. A final degas was made under vacuum after connection of the water reservoir to the vacuum system. The melanin films were initially placed under vacuum (< 0.01 mbar) and their reflectivity profiles were recorded. Samples were then exposed to the desired pressure of H_2O or D_2O vapour (regulated

by the sorption/desorption system) and their reflectivity profiles were recorded. The sample chamber was then evacuated to purge the atmosphere and observe the reversibility of the sorption process before the next exposure to H_2O or D_2O (Figure S2). The pressure in the sample chamber was observed to vary by around ± 0.3 mbar during the ~4-6 h exposures to H_2O and D_2O and this error range was ascribed to all exposure pressures. After changing the pressure within the cell, data was recorded with $Q \in [0.008, 0.057]/Å^{-1}$ (θ = 0.65º) at 600 s intervals. When three successive measurements yielded the same reflectivity profile the sample was deemed to be equilibrated and the reflectivity profile was recorded across the entire *Q*-range [0.008, 0.235]/$Å^{-1}$ (θ = 0.65º and 3.00º). Films were exposed to 0%, 7.5%, 20%, 50% and 80% of the saturation pressures of H_2O and D_2O, which were taken to be 31.0 mbar and 27.0 mbar, respectively.[40] It is important to note that the different absolute vapour pressures for H_2O and D_2O corresponding to each relative humidity (% of saturation pressure) result from the different saturation pressures of H_2O and D_2O and not from a change in temperature. The films were found to equilibrate within 20-50 mins after water exposure or evacuation. Reflected beam profiles for the equilibrated films were collected at 0.65º for 1200-1800 s and 3.0º for 5400-7200 s and normalised to direct beam profiles recorded for each reflection angle.

NR data modelling: Processing and analysis of the reflectivity profiles was performed using the Motofit reflectometry analysis program.[37, 43] All of the models described used an SLD of 2.07×10^{-6} $Å^{-2}$ for the silicon substrate. A three-layer model was used to fit all of the NR data and the justification for this is as follows. Initial modelling of the melanin films as a single layer on top of a thin SiO_2 layer (SLD = 3.47×10^{-6} $Å^{-2}$) led to unsatisfactory fits of poor visual quality with high χ^2 values. Additional layers were therefore added to the model to improve the fitting quality. Upon the addition of a second melanin layer, the modelling software reduced the SiO_2 thickness to zero, increased the interfacial roughness between Si and SiO_2 and placed a thin interfacial layer at either the air interface or the substrate interface with a slightly lower SLD than the bulk layer. It was often observed that the two-layer models would not converge to a unique solution as the χ^2 values for the two fits with the interfacial layer either at the air or substrate interface were very similar. To address this, the melanin layers were modelled as three-layer films comprising a bulk layer (which comprises the majority of the film) with two thin interfacial layers at the substrate and air interfaces. Such a model permits a transition layer at each interface. Once again, the fitting software minimised the thickness of the SiO_2 layer and increased the roughness between the silicon substrate and the lowest melanin layer. Given that the modelled SLDs of the interfacial layers in contact with the substrate are similar to or greater than the SiO_2 SLD it was concluded that the SiO_2 layer could not be adequately distinguished as a separate layer and it was removed from the model with its effects being incorporated into the increased roughness of the silicon/melanin interface. When the melanin

films were fitted using the three-layer model without a dedicated SiO_2 layer, it was found that several of the fitting parameters (the thickness and roughness of the interfacial layers and the substrate/melanin roughness) were practically invariant in each fit for a given film. As such, these parameters were fixed in the modelling based on the parameters from the best fit to the initial melanin films under vacuum [the 0.0 mbar plots in Figures 2 (A)-(D)] and a list of the parameters used is given in Tables S1 and S2 in the supplementary information. This left only four free structural modelling parameters – the thickness of the bulk melanin layer and the SLDs of the three melanin layers in the model. For modelling consistency, all NR profiles were modelled using the three-layer model with only four unconstrained parameters as described. This approach consistently gave the lowest χ^2 values (significantly lower than two layers), with excellent fits for all changes occurring for a given film during exposure to H2O or D2O and subsequent evacuation (representing a minimum of five SLD contrasts between the melanin film, air and the silicon substrate). This model also provided the flexibility for the modelling software to make the SLDs of the interfacial layers equal to that of the bulk layer if additional layers were not required (see Tables S1 and S2). In each case, the SLD of the interfacial layers rose and fell with the same trend as the bulk layer suggesting that water penetrating or leaving the bulk was also doing so in the interfacial layers.

X-ray reflectometry (XRR) measurements were performed as a function of incident angle (θ) on a Panalytical X'Pert Pro reflectometer operating with Cu Kα (1.54 Å) radiation. X-rays from a (45 kV) tube source were focused with a Göbel mirror, collimated with a 1/32º pre-sample slit and detected with a Xe scintillator detector. A sample was placed inside a custom-built sample chamber under a vacuum (16 mbar) for the measurement. Analysis of the reflectivity profile in Figure 1 (B) was also performed using the Motofit reflectometry analysis program.[37] The model used an SLD of 20.1×10^{-6} Å^{-2} (iSLD = 4.7×10^{-7} Å^{-2}) for the silicon substrate with an interfacial roughness of 6.3 Å between the silicon substrate and the overlying organic layer, which had a thickness of 443 Å, an SLD of 13.4×10^{-6} Å^{-2} and a roughness of 11.1 Å at the organic/air interface.

X-ray photoelectron spectroscopy (XPS) measurements were performed using a Kratos Axis Ultra XPS Surface Analysis System with a monochromatic Al Kα X-ray source. Survey and high resolution scans were taken at 120 and 20 eV pass energies, respectively. The spectra were referenced to the binding energy of the N 1s peak of poly(9-vinylcarbazole) at 400.22 eV.[44] The XPS spectra were analysed using Casa XPS software. Atomic ratios for C, N and O were determined from the integrated areas under the C 1s, N 1s and O 1s peaks, respectively, using Shirley backgrounds for the peak modelling.

Results and Discussion

The SLD, ρ_i, of a material i is given by

$$r_i = \frac{r_{M,i} N_{\mathrm{Av}}}{M_i} \sum_j n_j b_j \circ \frac{1}{V_i} \sum_j n_j b_j, \qquad (1)$$

where $\rho_{M,i}$ is the mass density of species i, N_{Av} is Avogadro's number, M_i is the formula mass of species i, V_i is the molecular volume of species i, n_j is the number of atoms j in the molecular formula of species i, and b_j are their corresponding bound coherent neutron scattering lengths[36]. To establish the effect of water exposure on the melanin films, it was first necessary to determine the mass density and average empirical formula of a dry melanin film under vacuum. This was achieved using a combination of three methods: NR, XRR and XPS, following procedures described previously (Figures 1 and S1).[45] Three independent NR measurements on evacuated melanin films prepared under the same conditions [Figure 1 (A)] revealed film thicknesses of 420-443 Å. The neutron reflectivity profiles were modelled with three layers as described in the experimental section. Both of the thin interfacial layers had SLDs that were slightly lower than or equal to the bulk layer depending on the exposure state. To simplify the analyses that follow, the thickness-weighted average of the individual layer SLDs (ρ_{Film}, Tables S3 and S4) were determined. The average neutron SLDs for the three melanin films under vacuum prior to exposure were similar being 3.29, 3.34 and 3.32×10^{-6} Å^{-2} [Figure 1 (A)]. The range of the observed ρ_{Film} values (0.05×10^{-6} Å^{-2}) was used to account for random sample-to-sample variations between measurements on separate films by adding this value to the uncertainties in the layer SLDs generated by the fitting software. The combined errors in the layer SLDs were then propagated throughout subsequent calculations. For the XRR contribution to the determination of the prefactor in Equation (1), an X-ray reflectivity profile recorded for a fourth evacuated melanin film [Figure 1 (B)] was modelled as a single layer with a thickness of 443 Å and an X-ray SLD of 13.4×10^{-6} Å^{-2}. Finally, high-resolution XPS measurements under vacuum revealed atomic percentages for C, N and O of 72.3%, 9.2% and 18.5%, respectively (Figure S1). When combined with the neutron and X-ray SLDs these atomic ratios were consistent with the empirical formula (used to determine M_i) of $C_{7.83}H_{5.39}NO_{2.01}$, which is commensurate with that of crosslinked dihydroxyindole ($C_8H_7NO_2$) and indolequinone ($C_8H_5NO_2$), and a mass density ($\rho_{M,\mathrm{i}}$) of 1.52 g cm^{-3} for the initial melanin matrix under vacuum. Given that the XPS measurements were performed under vacuum and that the C:N:O ratios determined were commensurate with the known molecular constituents of melanin, it was assumed that most of the sorbed water was removed from the as-cast films under vacuum for the purposes of our analysis. Throughout this work the "matrix" is defined as the macromolecular melanin framework associated with the initial film volume. This includes voids associated with

imperfect packing of the macromolecules in the evacuated film and any water that sorbs into these voids upon exposing the film to water.

With the baseline material parameters ascertained, the effect of increasing pressures of H_2O or D_2O vapour are shown in the corresponding NR profiles given in Figures 2 (A) & (C), respectively. After each exposure to water vapour the sample chamber was evacuated and the reflectivity profiles of the films were re-measured to examine the reversibility of the sorption processes. The corresponding NR profiles of the evacuated films after each exposure are shown in Figures 2 (B) & (D) for H_2O and D_2O, respectively. The reflectometry profiles obtained were modelled as three-layer films as described for the initial film NR data in Figure 1. As described in the experimental section, the changes in the reflectivity profiles due to sorption and desorption of water were modelled with only four free structural parameters: the bulk layer thickness and the SLDs of the three layers in the model. A complete list of the fitting parameters used is given in Tables S1 and S2 in the supplementary information and the corresponding total film thicknesses and average film SLDs (ρ_{Film}s) are given in Tables S3 and S4. The fact that the exposed films could be modelled by simply expanding the bulk layer, yielding predominantly uniform SLD *versus* thickness plots, indicates a largely even distribution of H_2O or D_2O throughout the film volume.

Upon exposure to increasing vapour pressures of H_2O the melanin films were observed to swell [inset Figure 2 (A)] whilst the SLD of the film decreased, as was expected from the uptake of H_2O. For vapour pressures up to 6.2 mbar (20% relative humidity) of H_2O, the film was observed to contract to close to its original thickness and SLD upon evacuation. However, incomplete contraction was observed when the film was exposed to higher H_2O pressures [Figure S2 (A)]. The melanin film exposed to increasing vapour pressure of D_2O was observed to swell and contract in a similar manner to the film exposed to H_2O [Figure S3 (A)], with incomplete contraction observed after exposure to D_2O pressures of 13.6 mbar (50% relative humidity) and above. The SLD of the exposed film also increased significantly [Figure 2 (C)], as was expected from the uptake of D_2O into the film. The SLD of the evacuated film also rose after each successive exposure to D_2O [Figure 2 (D) inset], indicating that H-D exchange was occurring with the melanin macromolecules in the film. It was assumed that any additional volume of the films after swelling and evacuation (determined from the film thickness) was occupied by traces H_2O or D_2O trapped during contraction of the films with their usual neutron SLDs. The effects of water exposure on the melanin films were quantified by separating the contributions of the melanin matrix and the swelling water to the average film SLD using

$$\rho_{\text{Film}} = \phi_{\text{Matrix}}\rho_{\text{Matrix}} + \phi_{\text{Swelling}}\rho_{\text{Water}} \qquad (2)$$

$$\text{where } \phi_{\text{Swelling}} = \frac{T_{\text{Swollen}} - T_{\text{Initial}}}{T_{\text{Swollen}}}, \qquad (3)$$

$$\phi_{\text{Swelling}} + \phi_{\text{Matrix}} = 1, \qquad (4)$$

$$\rho_{\text{Matrix}} = \phi'_{\text{Melanin}}\rho_{\text{Melanin}} + \phi'_{\text{Voids}}\rho_{\text{Voids}} + \phi'_{\text{Water,Matrix}}\rho_{\text{Water}}, \qquad (5)$$

$$\text{and } \phi'_{Melanin} + \phi'_{Voids} + \phi'_{Water,Matrix} = 1, \qquad (6)$$

where ρ_{Film} is the average modelled SLD of the film, ρ_{Matrix} is the SLD of the melanin matrix, ρ_{Water} is the SLD of either H_2O (-0.56×10^{-6} Å^{-2}) or D_2O (6.36×10^{-6} Å^{-6}), ϕ_{Swelling} is the fraction of the film volume occupied by swelling water [that is > 0 for all exposed films and evacuated films that did not return to their original thickness, see Figures 4 (A) and (D)], ϕ_{Matrix} is the fraction of the swollen film volume that was occupied by the melanin film at its initial thickness T_{Initial}, T_{Swollen} is the thickness of the swollen film after water exposure, ϕ'_{Melanin} is the volume fraction of the matrix occupied by the melanin and ρ_{Melanin} is its corresponding SLD, ϕ'_{Voids} is the volume fraction of the matrix occupied by void space ($\rho_{\text{Voids}} = 0.00 \times 10^{-6}$ Å^{-2}), and $\phi'_{\text{Water,Matrix}}$ is the volume fraction of the matrix occupied by water that sorbs into the void space.

In Equations (2–6) the matrix is defined by the initial volume occupied by the melanin film under vacuum prior to water exposure, incorporating any voids associated with imperfect packing of the melanin. During water exposures some of the void space becomes occupied by matrix water (in addition to the swelling water accounted for by $\phi_{\text{Swelling}}\rho_{\text{Water}}$) and ρ_{Matrix} comprises SLD contributions from the melanin, the void space and any water occupying the voids. These are represented by the $\phi'_{\text{Melanin}}\rho_{\text{Melanin}}$, $\phi'_{\text{Voids}}\rho_{\text{Voids}}$ and $\phi'_{\text{Water,Matrix}}\rho_{\text{Water}}$ terms, respectively. Henceforth, water contributing to the ϕ_{Swelling} term will be referred to as "swelling water" and water contributing to the $\phi'_{\text{Water,Matrix}}$ term will be referred to as "matrix water".

To begin the analysis of water uptake, the values of ϕ_{Swelling} were determined during (exposed) and after (evacuated) exposure to increasing H_2O and D_2O pressures using Equation (3) and their values are shown in Figures 3 [(A), H_2O] and [(D), D_2O], respectively. The volume fractions due to swelling water were up to 0.19 for H_2O exposure and 0.17 for D_2O exposure. The small residual volume occupied by swelling water in the evacuated films following exposure to high pressures was found to be up to 0.02 for the film exposed to H_2O and up to 0.04 for the film exposed to D_2O and H_2O. It was found that ϕ_{Swelling} was proportional to the absolute exposure pressure [Figure 4 (A)], regardless of whether the film was exposed to H_2O or D_2O. This indicated a direct relationship between melanin film swelling and the number of water molecules in the atmosphere, and not the relative humidity as might be expected from Raoult's law.

To determine the effects of exposure on the matrix, the SLDs of the melanin matrix (ρ_{Matrix}) were calculated from ϕ_{Swelling} and ρ_{Film} using Equations (4) and (2) and these are plotted as a function of

exposure state for exposed and evacuated melanin films in Figures 3 (B, H_2O) and (E, D_2O). In the case of H_2O exposure, the value of ρ_{Matrix} was constant (within error) for all exposure states. This indicates that the volume fractions of melanin molecules ($\phi'_{Melanin}$) and the sum of the voids (ϕ'_{Voids}) and matrix water ($\phi'_{Water,Matrix}$) did not change significantly upon expansion and contraction under H_2O, once the small contributions from swelling water to the film SLD ($\phi_{Swelling}\rho_{Water}$) were removed. Given that the SLD contribution of matrix H_2O would be negligibly small it was not possible to separate it from the SLD contribution of the void space of 0 $Å^{-2}$. Nevertheless, the invariance of ρ_{Matrix} with H_2O exposure state indicates that the partial molar volume of the melanin molecules was unaltered upon expansion and contraction. In contrast, the values of ρ_{Matrix} for the film exposed to D_2O were not constant but followed the same trend as ρ_{Film} once the contributions from the swelling D_2O had been removed. Exposure to D_2O led to significant increases in ρ_{Film} and ρ_{Matrix}, in part because of the relatively large positive SLD of the D_2O swelling the film. The increases of ρ_{Matrix} on exposure to D_2O could result from changes in the amount of sorbed matrix water or changes in the SLD of the melanin molecules upon H/D-exchange [Equation (5)] and so an examination of these effects was undertaken.

To quantify water uptake into the matrix, and thereby the total water uptake of the melanin films, it was necessary to determine the amount of swelling water and the amount of matrix water in the film upon exposure. This involved separating the contributions of the melanin, matrix water, swelling water and voids to ρ_{Film} [Equations (2) and (5)], which will now be discussed. The SLD contribution of the matrix ($\phi_{Matrix}\rho_{Matrix}$) and ρ_{Film} for the exposed films are plotted in Figure 4 (B) to indicate the contribution of the swelling water ($\phi_{Swelling}\rho_{Water}$) to ρ_{Film}. The values of $\phi_{Swelling}\rho_{Water}$ for H_2O were an order of magnitude less and of opposite sign than those for D_2O due to the relative values of ρ_{Water} being -0.56×10^{-6} $Å^{-2}$ and 6.36×10^{-6} $Å^{-6}$, respectively. This meant that within the experimental error $\rho_{Film} \approx \phi_{Matrix}\rho_{Matrix}$ in the case of H_2O exposure, making the SLD contribution from matrix H_2O too small to be determined. We therefore focussed on the D_2O exposure data to determine the uptake of D_2O into the voids in the melanin matrix. Since the exchange of labile protons in the melanin macromolecules for deuterons (H/D-exchange) was expected based on the comproportionation equilibrium (Scheme 1), the value of ρ_{Matrix} was expected to increase with D_2O exposure pressure due to increases in $\rho_{Melanin}$. As previously described, it was assumed that any additional volume in the evacuated film after exposure to higher D_2O pressures [Figure 3 (D)] was caused by residual swelling D_2O trapped in the film by rapid contraction of the expanded matrix towards its original volume. The SLDs of the melanin matrix (ρ_{Matrix}) for both the D_2O exposed and subsequently evacuated films are plotted against exposure pressure in Figure 5 (A). It was found that the ρ_{Matrix} curves for the exposed and subsequently evacuated melanin matrix did not overlap, with the value of ρ_{Matrix} for the film exposed to D_2O being greater than the subsequently evacuated

film in each case. Both curves were fitted using a Type I isotherm[46] (details of which will follow shortly) consistent with chemisorption of the D_2O into voids within the melanin matrix, followed by subsequent desorption of this bound water upon evacuation of the films. Therefore, the increase in ρ_{Matrix} of the evacuated film (with respect to the initial ρ_{Matrix}) with each D_2O exposure pressure was attributed to H/D-exchange between D_2O and the melanin [red shaded area in Figure 5 (A), under the assumption that all matrix water was removed from the voids upon evacuation]. The additional contribution to ρ_{Matrix} in the exposed film [blue shaded area in Figure 5 (A)] was attributed to matrix D_2O occupying the inherent voids within the matrix that was subsequently removed under vacuum. In light of the observation that ρ_{Matrix} was constant for the melanin film exposed to H_2O [Figure 3 (B)], it seems clear that the volume fraction of melanin within the matrix ($\phi'_{Melanin}$) remained relatively constant whether the film was evacuated or exposed. The volume fraction of the matrix occupied by water ($\phi'_{Water,\ Matrix}$) was therefore estimated by extension of equation (5) to give

$$\rho_{Matrix,Exposed} = \phi'_{Melanin}\rho_{Melanin} + \phi'_{Voids,Exposed}\rho_{Voids} + \phi'_{Water,Matrix}\rho_{Water}, \qquad (7)$$

$$\rho_{Matrix,Evacuated} = \phi'_{Melanin}\rho_{Melanin} + \phi'_{Voids,Evacuated}\rho_{Voids}, \qquad (8)$$

$$\text{where } \phi'_{Voids,Evacuated} = \phi'_{Voids,Exposed} + \phi'_{Water,Matrix}, \qquad (9)$$

$$\text{and } \phi'_{Water,Matrix} = \frac{\rho_{Matrix,Exposed} - \rho_{Matrix,Evacuated}}{\rho_{Water}}, \qquad (10)$$

where $\rho_{Matrix,Exposed}$ and $\rho_{Matrix,Evacuated}$ are the ρ_{Matrix} values for the exposed and subsequently evacuated melanin film for a given exposure pressure [Figure 5 (A)], $\rho_{Melanin}$ is the SLD of the melanin macromolecules at a given exposure pressure (reflecting the level of H/D-exchange), $\rho_{Voids} = 0.00 \times 10^{-6}$ Å^{-2}, and $\rho_{Water} = 6.36 \times 10^{-6}$ Å^{-2} for D_2O. It should be noted from Equation (10) that the invariance of ρ_{Matrix} upon exposure to H_2O and subsequent evacuation [Figure 3 (B)] precluded the determination of $\phi'_{H_2O,\ Matrix}$ for the film exposed to H_2O. The values of $\phi'_{D_2O,\ Matrix}$ calculated using Equation (10) are shown in Figure 5 (B) and a considerable fraction of the matrix volume [$\phi'_{D_2O,\ Matrix} = 0.11 \pm 0.02$] was found to be occupied by D_2O at 80% relative humidity.

Given that it was assumed that the increases in $\rho_{Matrix,Evacuated}$ were due primarily to H/D-exchange, this was quantified as the percentage of exchanged H nuclei using Equation (1). The number density of melanin units of average molecular formula $C_{7.83}H_{5.39}NO_{2.01}$ was determined from the product of their initial number density [prefactor in Equation (1)] in the melanin film prior to D_2O exposure (6.28×10^{-3} Å^{-3}) and ϕ_{Matrix} of the deuterated films under vacuum to account for the slight film expansion upon exposure to higher D_2O pressures. By exchanging H nuclei ($b_H = -3.74$ fm)[36] for D nuclei ($b_D = 6.67$ fm)[36] in the summation term of Equation (1) it was found that up to 47% of the melanin protons were exchanged for deuterons as the D_2O exposure pressure was increased to 21.6 mbar (80% relative humidity) [Figure 5 (B), red curve]. It should be noted

that this calculation provides an upper limit for the amount of H/D-exchange because it was assumed that all of the matrix D_2O could be removed upon evacuation of the sample chamber. If this assumption was modified to permit a degree of matrix water to be trapped, like the swelling water was found to be at higher exposure pressures, this would also increase the observed values of ρ_{Matrix} in the evacuated state. To provide an estimate of the amount of matrix water that may be trapped in the evacuated films, the fraction of swelling water remaining in the films after exposure and evacuation [$\phi_{Swelling,Evacuated}/\phi_{Swelling,Exposed}$] was calculated for each exposure pressure. The equivalent SLD contribution from residual trapped matrix D_2O was calculated assuming that the same fraction of matrix D_2O [Figure 5 (B)] was trapped in the film after evacuation at each exposure pressure. The SLD contribution from this additional trapped matrix D_2O was subtracted from the observed values of ρ_{Matrix} for the evacuated film at each exposure pressure to give the black curve in Figure 5 (A). The corresponding percentage deuteration values after removing the contribution from additional trapped matrix D_2O [Figure 5 (B)] indicate a maximum percentage deuteration of around 42% after the 21.4 mbar D_2O exposure, indicating that the assumption of complete matrix water removal may overestimate the amount of deuteration by around 5% at higher exposure pressures. This suggests that 42-47% of the hydrogens in melanin are available for exchange in the comproportionation reaction (Scheme 1). Given the chemically amorphous nature of the melanin matrix it was not possible from these measurements to say which H nuclei were being exchanged. However, given the rate at which this occurs that the predominant exchange would be OH and NH exchange as opposed to CH exchange.

The pressure dependences of both the percentage of H/D-exchange and the $\phi'_{D_2O,Matrix}$ values follow the shape of a type 1 isotherm. We therefore modelled the data with:

$$f(p) = \frac{n\alpha p}{1+\alpha p}, \qquad (11)$$

where n is the limiting value of $f(p)$ at infinite pressure, α is a constant related to the strength of adsorption and p is the absolute pressure of D_2O over the film. The α parameters determined by least squares fitting to the data were the same within experimental error, being 0.12 ± 0.01 and 0.07 ± 0.05 mbar^{-1} for the H/D-exchange percentage and $\phi'_{D_2O,Matrix}$, respectively. This may indicate some correlation between the two processes: as the pressure rises the amount of internal surface area covered with chemisorbed D_2O increases according to Equation (11); H/D-exchange then occurs with the matrix D_2O causing the extent of melanin deuteration to follow a similar trend. For this mechanism to be consistent with our experimental observations, it would require a relatively a slow exchange of the water within the film with the remaining water in the sample chamber in order to be consistent with the stability of the film reflectometry profiles over the 2–2.5 hour

measurement period (otherwise the reflectivity profiles recorded at the two reflection angles would not overlap). That is, the exchanged hydrogen atoms do not appear to escape the film within the experimental timeframe but only upon evacuation of the film.

Having quantified the influence of swelling water, matrix water and H/D-exchange on ρ_{Film}, the only compositional parameter remaining is the intrinsic void space within the melanin matrix. Given that the voids have no scattering length density ($\rho_{\text{Voids}} = 0$ Å^{-2}) it was not possible to measure their volume fraction directly. However, the maximum volume fraction of the matrix occupied by D_2O at infinite exposure pressure [n in equation (11)] was estimated to be 0.18 ± 0.07 and this represents a lower limit estimate for ϕ'_{Voids} within the melanin matrix.

To draw the above analysis together, the total contribution of D_2O to the measured SLD of the film exposed to D_2O ($\rho_{\text{Water,Film}}$) was determined using

$$\rho_{\text{Film}} = \phi_{\text{Matrix}}(\phi'_{\text{Melanin}}\,\rho_{\text{Melanin}} + \phi'_{\text{Voids}}\,\rho_{\text{Voids}} + \phi'_{\text{Water,Matrix}}\,\rho_{\text{Water}}) + \phi_{\text{Swelling}}\rho_{\text{Water}}, \qquad (12)$$

$$\rho_{\text{Water,Film}} = (\phi_{\text{Swelling}} + \phi_{\text{Matrix}}\phi'_{\text{Water,Matrix}})\rho_{\text{Water}}. \qquad (13)$$

The individual contributions from swelling D_2O and matrix D_2O from Equation (13) are shown in Figure 6 (A) along with the total $\rho_{\text{Water,Film}}$. The summation of the contributions from matrix (Type I isotherm behaviour with p) and swelling (linear behaviour with p) D_2O leads to an almost linear increase in the contribution of D_2O to the SLD of the film following the initial rapid intake of water into the matrix voids. The SLD contributions of D_2O and melanin were converted into the corresponding adsorption isotherm for comparison with the previously reported gravimetric isotherm for the sorption of D_2O into melanin pellets.[15] The molar density of D_2O (in mol cm^{-3}) was determined from $\rho_{\text{Water,Film}}$ and $\sum_j n_j b_j$ (= 1.91×10^{-4} Å^{-2} for D_2O) using Equation (1). Similarly, the mass density of melanin (in g cm^{-3}) was determined from the SLD of the swollen deuterated matrix (= $\phi_{\text{Matrix}}\rho_{\text{Matrix,Evacuated}}$) and the corresponding $\sum_j n_j b_j$ and M_i values for the appropriate level of H/D-exchange at each D_2O exposure pressure. The corresponding isotherm was then determined by dividing the molar density of D_2O by the mass density of melanin within the film [Figure 6 (B)]. It should be noted that the isotherm determined from the NR data takes into account the effect of H/D-exchange on the melanin mass, whereas the gravimetric isotherm does not. However, the minor differences in mass densities of the H/D-exchanged matrix and the matrix with natural isotopic abundance of 0.01–0.04 g cm^{-3} were all within the experimental errors in the calculated density values of 0.05–0.06 g cm^{-3}.

The thin film isotherm indicated D_2O uptakes on the same order of magnitude as the previously reported gravimetric isotherm for pellets. Furthermore, the curves appear to have a similar form with the rapid Type I isotherm uptake of D_2O into the voids dominating at low pressures followed

by a more linear film swelling regime at higher pressures. The gravimetric isotherm for the uptake of D_2O by pelletised melanin appears to contain a much greater contribution from the Type I isotherm behaviour indicative of more pronounced uptake of D_2O into voids in the matrix. We correlate this observation with the larger interfacial area of the pelletised samples and the fact that the melanin within them is likely to be less well packed than the compact thin films. This observation is also consistent with the generally lower uptake of D_2O by the thin film samples. At higher exposure pressures the isotherms show similar gradients of D_2O uptake with increasing pressure indicating consistent uptake of swelling water in pellets and thin films after the void space becomes largely saturated with matrix water.

To complete the study, a final measurement was performed to probe the reversibility of H/D-exchange with the melanin matrix. After the 21.4 mbar D_2O exposure (80% relative humidity) and subsequent evacuation, the ρ_{Film} of $(4.80 \pm 0.07) \times 10^{-6}$ Å^{-2} was larger than the initial ρ_{Film} prior to D_2O exposure of $(3.34 \pm 0.05) \times 10^{-6}$ Å^{-2}, due to the H/D-exchange between D_2O and the melanin molecules. The film was then subjected to a single exposure of 24.8 mbar (80% relative humidity) H_2O (Figure 7) without breaking the vacuum in the sample chamber.. Upon exposing the deuterated melanin film to the same relative humidity of H_2O and allowing it to equilibrate, the fringes in the reflectivity profile had a much smaller amplitude. This indicated that the SLD of the film was approaching that of the silicon substrate in a similar manner to that observed for the film exposed to H_2O alone [Figure 2 (A)]. After subsequent evacuation, the SLD of the melanin film [$(3.47 \pm 0.05) \times 10^{-6}$ Å^{-2}] was nearly restored to its original value, indicating that exposure to H_2O was capable of reversing the H/D-exchange in the film. The interactions of water with melanin were therefore observed to be quasi-reversible both in a sense of swelling hysteresis and H/D exchange of labile melanin protons/deuterons upon raising and lowering the ambient water pressure.

With the above analysis concluded, we now turn to the relevance of the observations to the application of melanin thin films in device configurations. The key insights from the NR study in this regard are: firstly, around half of the melanin protons are labile and available for H/D-exchange; secondly, the predominantly uniform film SLD profiles indicate that melanin films absorb water evenly throughout their volume; and thirdly, the melanin film absorbs D_2O at similar magnitudes as previously published adsorption isotherms on pellets, with a near-linear increase with pressure after an initially rapid uptake. The large number of labile protons available in the film is an encouraging sign for ionic-electronic transduction. Considering the comproportionation reaction in Scheme 1, the generation of hydronium/deuteronium ions requires labile protons/deuterons. Thus, the combination of ready and reversible H/D-exchange shown above indicates that there are plentiful protons available for charge carrier generation. However, it must also be borne in mind that other proton sinks and sources are also present, such as amines and carboxylic acid groups that

do not take part in the redox process. Thus, we can expect melanin films to become more conductive as they are hydrated, which has been demonstrated.[13, 15, 19, 22, 23, 35]

Importantly, it has been shown previously that the water content in a melanin sample is not proportional to the relative humidity of water vapour above the melanin pellets.[15, 35] The NR data shows that the D_2O content in a melanin film is nearly proportional to the absolute vapour pressure above around 5 mbar as the Type 1 isotherm governing the sorption of D_2O into matrix voids begins to plateau and the linear contribution of the swelling water dominates the sorption profile [Figure 6 (A)]. This will simplify the analysis of future experiments by using the absolute exposure pressure, which is easily measured, as a surrogate for water content when correlating changes in other dependant variables above this exposure pressure. A further question remains as to whether this trend holds for H_2O vapour exposure. The gravimetric isotherms for H_2O and D_2O sorption by pellets are similar but the rapid initial rise in water content, which we correlate with the chemisorption of matrix water by the pellets, is less pronounced at low relative pressures of H_2O.[23] Combining this with the similar swelling behaviour of melanin films exposed to H_2O and D_2O [Figures 3 (A) and (D)] we expect that the adsorption isotherm for melanin thin films exposed to H_2O would also follow a near-linear trend akin to the D_2O isotherm in Figure 6 (B).

Conclusions

Melanin is an important biological functional material, which is proposed to be useful for bioelectronic interfaces because of its hybrid ionic/electronic conduction. The structural impact of water sorption on melanin films as a function of pressure has been observed for the first time using neutron reflectometry. The technique for controlling the vapour pressures eliminates common systematic errors found in studies that use saturated salt solutions as the water vapour source and opens up the technique for future research on water-sensitive conductive organic materials. Melanin thin films swell under water exposure, contract under subsequent evacuation and sorb both H_2O and D_2O evenly throughout the bulk. Furthermore, the D_2O sorption process is made up of two contributions: chemisorption into intrinsic voids in the film (matrix water) that follows a Type I isotherm and absorbed D_2O that leads to the expansion of the film volume (swelling water) that increases linearly with exposure pressure. When these contributions are considered together, the increase in total water content of the film is near-linear with D_2O exposure pressure. Reversible H/D-exchange with the melanin matrix revealed that nearly half of the melanin protons are labile and thereby available for charge conduction. All of these results combined with latent biocompatibility make melanin an excellent material choice for use in thin film bioelectronic devices.

Acknowledgements

This work was supported by an Australian Research Council Discovery Program DP120101372. MS is supported by a University of Queensland International Postgraduate Research Scholarship. PLB is a University of Queensland Vice Chancellor's Research Focused Fellow and PM is an ARC Discovery Outstanding Research Award Fellow. We acknowledge funding from the University of Queensland (Strategic Initiative, Centre for Organic Photonics & Electronics) and the Queensland Government (National and International Research Alliances Program). We also acknowledge the support of the Australian Centre for Neutron Scattering (formerly the Bragg Institute at the time of the NR/XRR experiments), the Australian Nuclear Science and Technology Organisation (ANSTO), and the Australian Institute for Nuclear Science and Engineering (AINSE) in providing the neutron research facilities used in this work. This work was performed in part at the Queensland node of the Australian National Fabrication Facility (ANFF), a company established under the National Collaborative Research Infrastructure Strategy to provide nano- and microfabrication facilities for Australian researchers. The authors acknowledge the facilities, and the scientific and technical assistance, of the Australian Microscopy & Microanalysis Research Facility at the Centre for Microscopy and Microanalysis, The University of Queensland. The authors would particularly like to thank Dr Barry Wood for his ever invaluable guidance with XPS measurements and analysis.

References

1. G. Prota, *Melanins and Melanogenesis*; Academic Press: San Diego CA, 1992.
2. P. Meredith and T. Sarna, *Pigm. Cell Res.*, 2006, **19**, 572-594.
3. V. Gray-Schopfer, C. Wellbrock and R. Marais, *Nature*, 2007, **445**, 851-857.
4. F. A. Zucca, G. Giaveri, M. Gallorini, A. Albertini, M. Toscani, G. Pezzoli, R. Lucius, H. Wilms, D. Sulzer, S. Ito, K. Wakamatsu and L. Zecca, *Pigm. Cell Res.*, 2004, **17**, 610-617.
5. W. D. Bush, J. Garguilo, F. A. Zucca, A. Albertini, L. Zecca, G. S. Edwards, R. J. Nemanich, and J. D. Simon, *PNAS USA*, 2006, **103**, 14785-14789.
6. A. A. R. Watt, J. P. Bothma and P. Meredith, *Soft Matter*, 2009, **5**, 3754-3760.
7. G. W. Zajac, J. M. Gallas, J. Cheng, M. Eisner, S. C. Moss, A. E. Alvarado-Swaisgood, *Biochim. Biophys. Acta*, 1994, **1199**, 271-278.
8. P. Meredith, B. J. Powell, J. Riesz, S. P. Nighswander-Rempel, M. R. Pederson and E. G. Moore, *Soft Matter*, 2006, **2**, 37-44.
9. M. L. Tran, B. J. Powell and P. Meredith, *Biophys. J.*, 2006, **90**, 743-752.
10. M. S. Blois, The Melanins: Their Synthesis and Structure. In *Photoch. Photobio. Rev.* Springer US, New York, 1978, Vol. 3, pp 115-135.
11. C. C. Felix, J. S. Hyde, T. Sarna and R. C. Sealy, *J. Am. Chem. Soc.*, 1978, **100**, 3922-3926.
12. P. J. Goncalves, O. B. Filho and C. F. O. Graeff, *J. Appl. Phys.*, 2006, **99**, 104701.
13. A. B. Mostert, B. J. Powell, F. L. Pratt, G. R. Hanson, T. Sarna, I. R. Gentle, and P. Meredith, *PNAS USA* 2012, **109**, 8943-8947.
14. A. B. Mostert, G. R. Hanson, T. Sarna, I. R. Gentle, B. J. Powell, and P. Meredith, *J. Phys. Chem. B*, 2013, **117**, 4965-4972.
15. S. B. Rienecker, A. B. Mostert, G. Schenk, G. R. Hanson, and P. Meredith, *J. Phys. Chem. B*, 2015, **119**, 14994-15000.
16. E. Dadachova, R. A. Bryan, X. Huang, T. Moadel, A. D. Schweitzer, P. Aisen, J. D. Nosanchuk and A. Casadevall, *PLoS ONE*, 2007, **2**, e457.
17. J. Riesz, J. Gilmore and P. Meredith, *Spectrochim. Acta A*, 2005, **61**, 2153-2160.
18. P. Meredith and J. Riesz, *Photochem. Photobiol.*, 2004, **79**, 211-216.
19. A. B. Mostert, B. J. Powell, I. R. Gentle and P. Meredith, *Appl. Phys. Lett.* 2012, **100**, 093701.
20. M. R. Powell and B. Rosenberg, *Bioenergetics*, 1970, **1**, 493-509.
21. M. Jastrzebska, H. Isotalo, J. Paloheimo and H. Stubb, *J. Biomat. Sci-Polym Ed.*, 1995, **7**, 577-586.
22. J. Wünsche, Y. Deng, P. Kumar, E. Di Mauro, E. Josberger, J. Sayago, A. Pezzella, F. Soavi, F. Cicoira, M. Rolandi and C. Santato, *Chem. Mater.*, 2015, **27**, 436-442.
23. J. Wünsche, F. Cicoira, C. F. O. Graeff and C. Santato, *J. Mater. Chem. B*, 2013, **1**, 3836-3842.
24. L. Glasser, *Chem. Rev.*, 1975, **75**, 21-65.
25. Y. J. Kim, W. Wu, S. Chun, J. F. Whitacre and C. J. Bettinger, *PNAS USA*, 2013, **110**, 20912-20917.
26. J. Rivnay, P. Leleux, M. Sessolo, D. Khodagholy, T. Herve, M. Fiocchi and G. G. Malliaras, *Adv. Mater.* 2013, **25**, 7010-7014.
27. M. Irimia-Vladu, *Chem. Soc. Rev.*, 2014, **43**, 588-610.
28. R. M. Owens and G. G. Malliaras, *MRS Bull.*, 2010, **35**, 449-456.
29. H. Lee, S. M. Dellatore, W. M. Miller and P. B. Messersmith, *Science* 2007, **318**, 426-430.
30. H. Lee, B. P. Lee and P. B. Messersmith, *Nature*, 2007, **448**, 338-342.
31. M. Abbas, F. D'Amico, L. Morresi, N. Pinto, M. Ficcadenti, R. Natali, L. Ottaviano, M. Passacantando, M. Cuccioloni, M. Angeletti and R. Gunnella, *Eur. Phys. J. E*, 2009, **28**, 285-291.
32. M. Ambrico, P. F. Ambrico, A. Cardone, T. Ligonzo, S. R. Cicco, R. Di Mundo, V. Augelli, and G. M. Farinola, *Adv. Mater.*, 2011, **23**, 3332-3336.
33. J. Bothma, J. de Boor, U. Divakar, P. Schwenn and P. Meredith, *Adv. Mater.*, 2008, **20**, 3539-3542.
34. M. P. da Silva, J. C. Fernandes, N. B. de Figueredo, M. Mulato and C. F. O. Graeff, *AIP Advances*, 2014, **4**, 037120.
35. A. B. Mostert, K. J. P. Davy, J. L. Ruggles, B. J. Powell, I. R. Gentle and P. Meredith, *Langmuir*, 2010, **26**, 412-416.
36. V. F. Sears, *Neutron News*, 1992, **3** (3), 26-37.
37. A. Nelson, *J. Appl. Crystallogr.*, 2006, **39**, 273-279.
38. S. C. DeCaluwe, P. A. Kienzle, P. Bhargava, A. M. Baker and J. A. Dura, *Soft Matter*, 2014, **10**, 5763-5776.
39. W. P. Kalisvaart, H. Fritzsche and W. Mérida, *Langmuir*, 2015, **31**, 5416-5422.

40. A. H. Harvey and E. W. Lemmon, *J. Phys. Chem. Ref. Data*, 2002, **31**, 173.
41. D. R. Lide, *CRC Handbook of Chemistry and Physics*, 86th ed.; Taylor & Francis: Boca Raton, Florida, 2005.
42. M. James, A. Nelson, S. A. Holt, T. Saerbeck, W. A. Hamilton and F. Klose, *Nucl. Instrum. Meth. A*, 2011, **632**, 112-123.
43. A. Nelson, *J. Phys. Conf. Ser.*, 2010, **251**, 012094.
44. G. Beamson and D. Briggs, *High Resolution XPS of Organic Polymers: The Scienta Esca300 Database*; John Wiley & Sons: Chichester, England, UK, 1992.
45. A. Nelson, B. W. Muir, J. Oldham, C. Fong, K. M. McLean, P. G. Hartley, S. K. Øiseth and M James, *Langmuir*, 2005, **22**, 453-458.
46. G. Barnes, and I. R. Gentle, *Interfacial Science: An Introduction*; Oxford University Press: Oxford, England, UK, 2005.

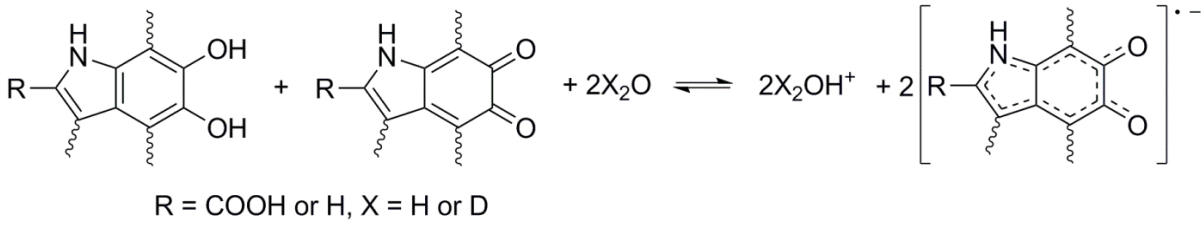

R = COOH or H, X = H or D

Scheme 1*: The comproportionation reaction between melanin and sorbed water. A dihydroxyindole and an indolequinone react with water to form indole semiquinone radical anions and hydronium cations. Wavy bonds indicate potential crosslinking sites between indole units.*

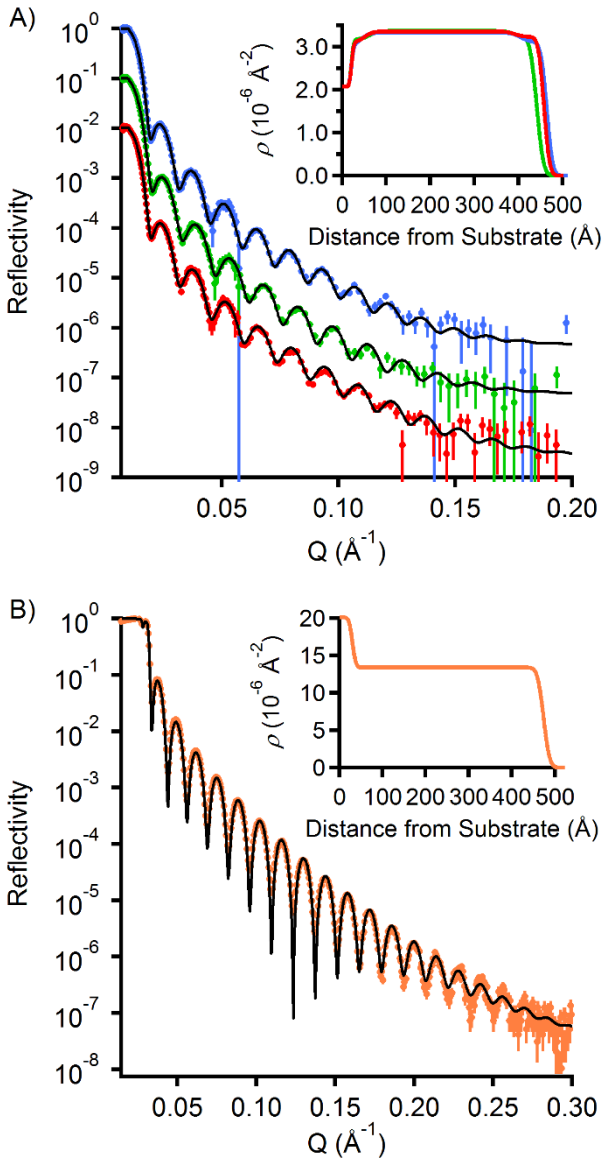

Figure 1 *(A) NR and (B) XRR profiles of melanin thin films dried under vacuum. Each data set was recorded on a separate film produced from the same melanin solution. Individual points indicate recorded data and solid lines black lines represent the spectrum predicted by the fitting model and traces are offset for clarity in (A). The insets show the corresponding modelled 1D variations in SLD with increasing distance from the silicon substrates.*

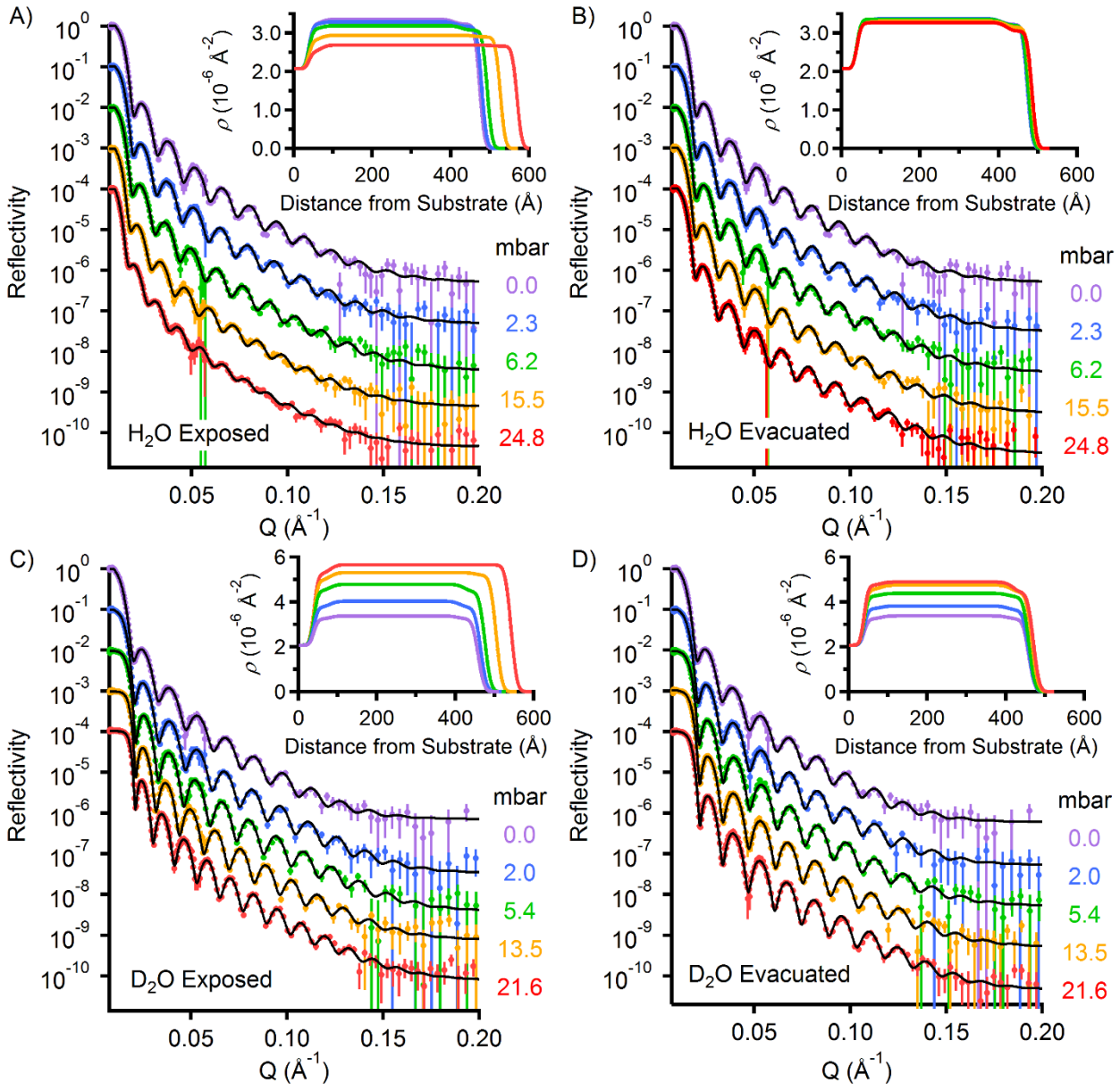

Figure 2 *NR profiles (offset for clarity) with fits and modelled SLD versus thickness plots (inset) for melanin films exposed to H_2O (A & B) and D_2O (C & D). All of the data in (A) and (B) are from measurements on the same film and all of the data in (C) and (D) were recorded on a separate film. In each figure the 0.0 mbar spectrum corresponds to the initial measurement of the film under vacuum. Figures (A) and (C) show the data for films exposed to H_2O and D_2O, respectively. Pressures are given in the legend on the right of each figure. Figures (B) and (D) show the data for films after the cell was evacuated following each exposure to remove the H_2O and D_2O, respectively.*

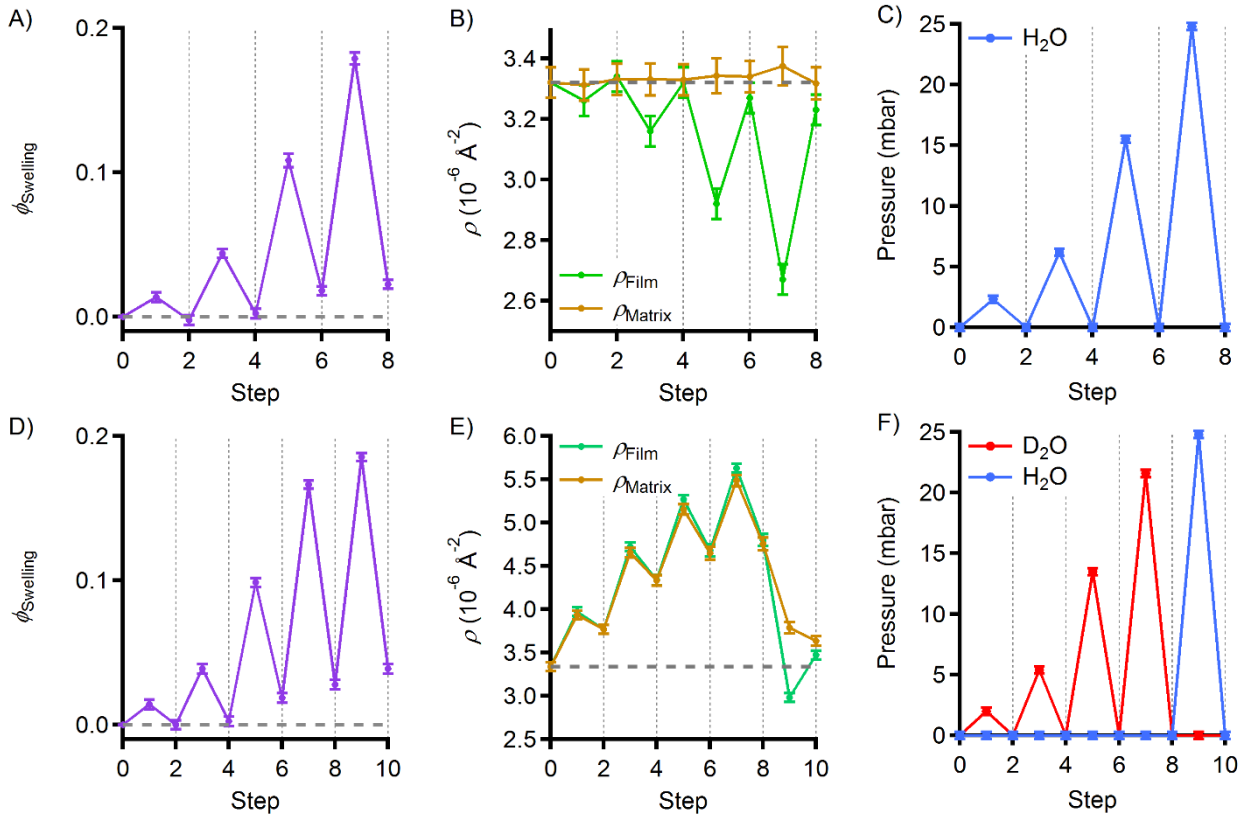

Figure 3 *Volume fraction and SLD parameters extracted from the model fits using Equations (2–4) for the films exposed to (A-C) H_2O and (D-F) D_2O followed by H_2O. (A) and (D) show the values of $\phi_{Swelling}$ determined from the initial and swollen film thicknesses, (B) and (E) show the average film SLDs and the SLD of the matrix determined by dividing $\phi_{Matrix}\rho_{Matrix}$ by ϕ_{Matrix} [= 1 − $\phi_{Swelling}$ in Figures (A) and (C)], and (C) and (F) show the exposure pressures to H_2O or D_2O at each step of the process.*

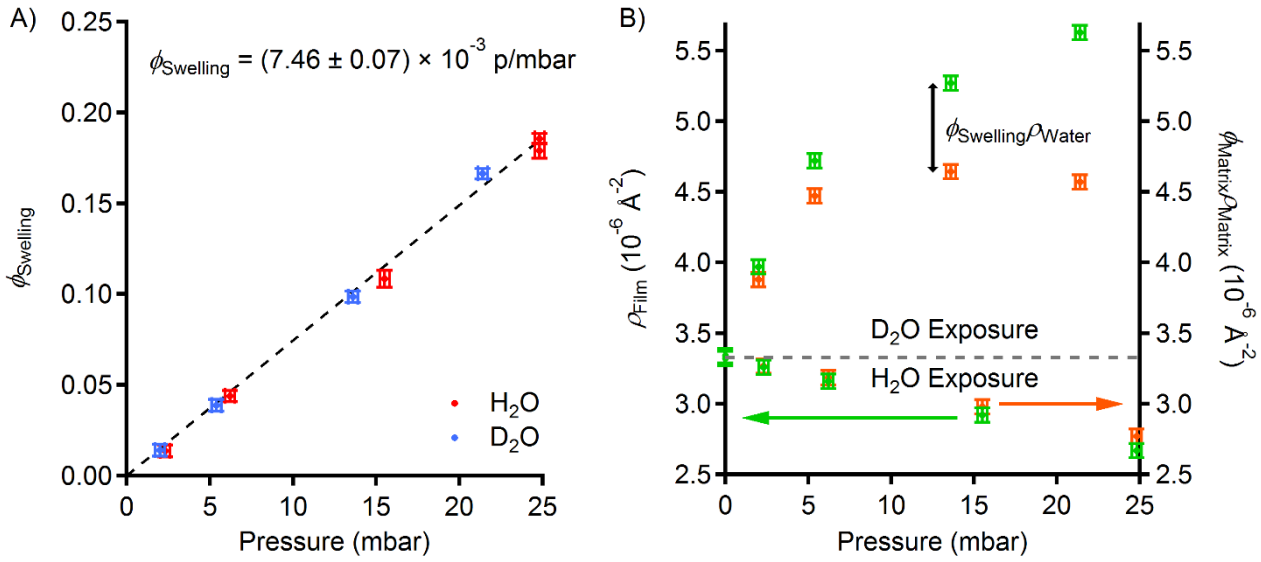

Figure 4 *(A) The calculated values of $\phi_{Swelling}$ upon exposure to H_2O (red) and D_2O (blue) plotted against exposure pressure. Twice the standard deviation (2σ) determined from the fitting model by Motofit (Tables S3 and S4) was used for the error in the total thickness of each sample and these errors were propagated using the chain rule when determining the values of $\phi_{Swelling}$. (B) The corresponding measured values of ρ_{Film} (green) and the calculated contribution of the matrix to this SLD ($\phi_{Matrix}\rho_{Matrix}$, orange) determined by subtracting the contribution from swelling water ($\phi_{Swelling}\rho_{Water}$) as in Equation (2). The grey dashed line in (B) indicates the initial film SLDs and delineates the regimes of the plot corresponding to H_2O (decreasing film SLD) and D_2O (increasing film SLD) exposure.*

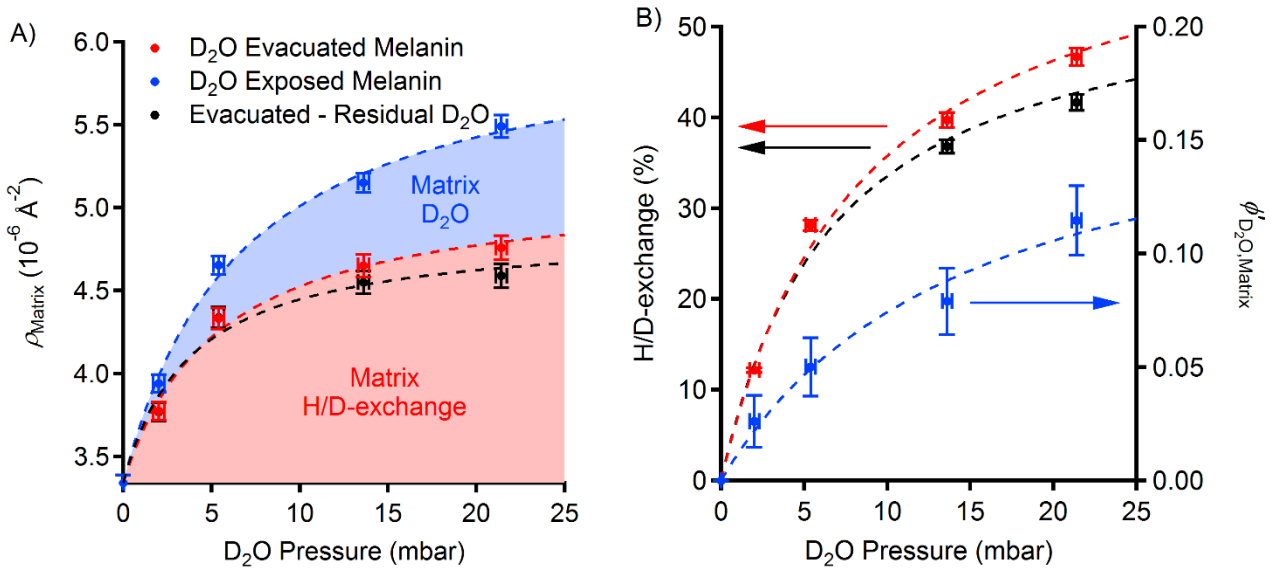

Figure 5 *(A) The values of ρ_{Matrix} for the film exposed to D_2O vapour and post evacuation, determined using Equation (2) from the values of $\phi_{Swelling}$ and ρ_{Film}. Both curves have been fitted to Type I isotherms. The blue curve indicates ρ_{Matrix} when the film was exposed to D_2O. The red curve indicates ρ_{Matrix} when the sample chamber was evacuated to remove the labile D_2O. The black curve indicates the predicted value of the ρ_{Matrix} for the evacuated film assuming that the same percentage of matrix D_2O was trapped in the film after evaporation as swelling D_2O. (B) The corresponding H/D-exchange percentage and the volume fraction of matrix D_2O occupying voids that leads to the difference in SLD observed in Figure 5 (A). H/D-exchange (red and black curves) is expressed as a percentage of the initial hydrogen stoichiometry required to give the SLD difference between the evacuated matrix SLDs and the initial matrix SLD. The volume fraction of matrix D_2O (blue curve) was calculated using Equation (10) and both curves are fitted to Type I isotherms.*

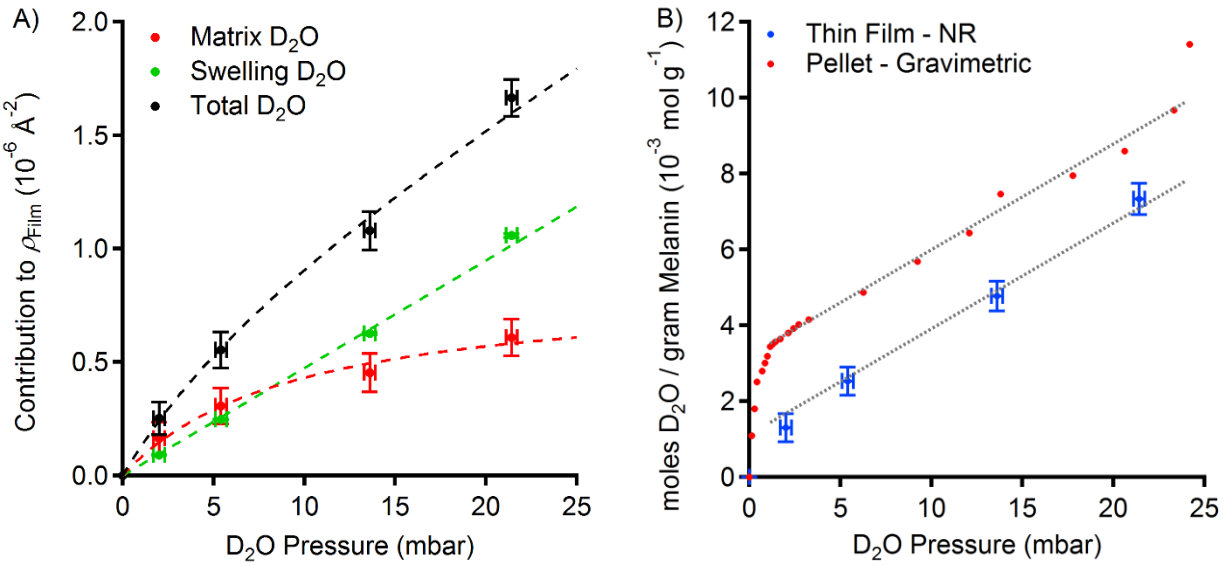

Figure 6 *(A) The contributions of D_2O to the SLD of the total exposed film SLD as a function of pressure. The total contribution (black) has been broken down into a contribution from D_2O causing the film to swell (green,* linear*) and D_2O chemisorbed into voids in the matrix (red,* type I isotherm*). (B) D_2O adsorption isotherms measured by neutron reflectometry (NR) and gravimetric methods.*[15] *The dashed grey lines in (B) follow the same gradient and are a guide to the eye.*

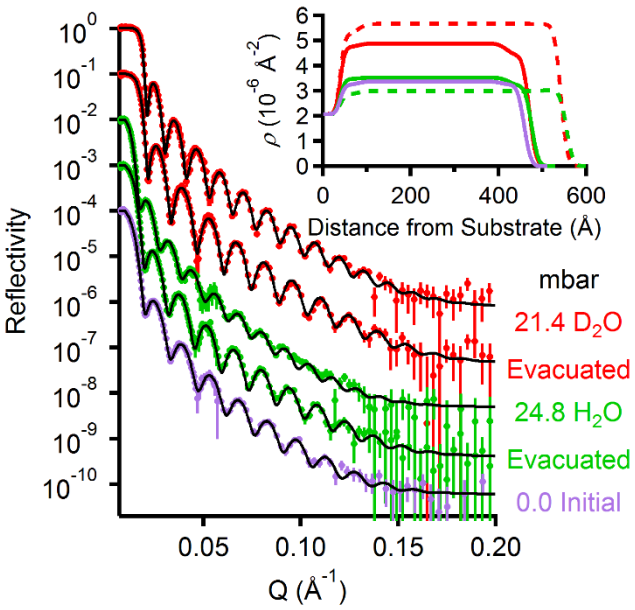

Figure 7 *NR profiles (offset for clarity) and SLD versus thickness profiles (inset) for the film initially exposed to D_2O [Figures 2 (C) and (D)] followed by a final exposure to H_2O. The upper four profiles show the results of successive exposures (followed by evacuation) to 80% relative humidity of D_2O (red) and H_2O (green). The bottom curve (purple) is the initial profile recorded for the film under vacuum before any exposures were made. In the inset the solid lines indicate the evacuated sample and the dashed lines the D_2O/H_2O-exposed sample.*

TOC Graphic

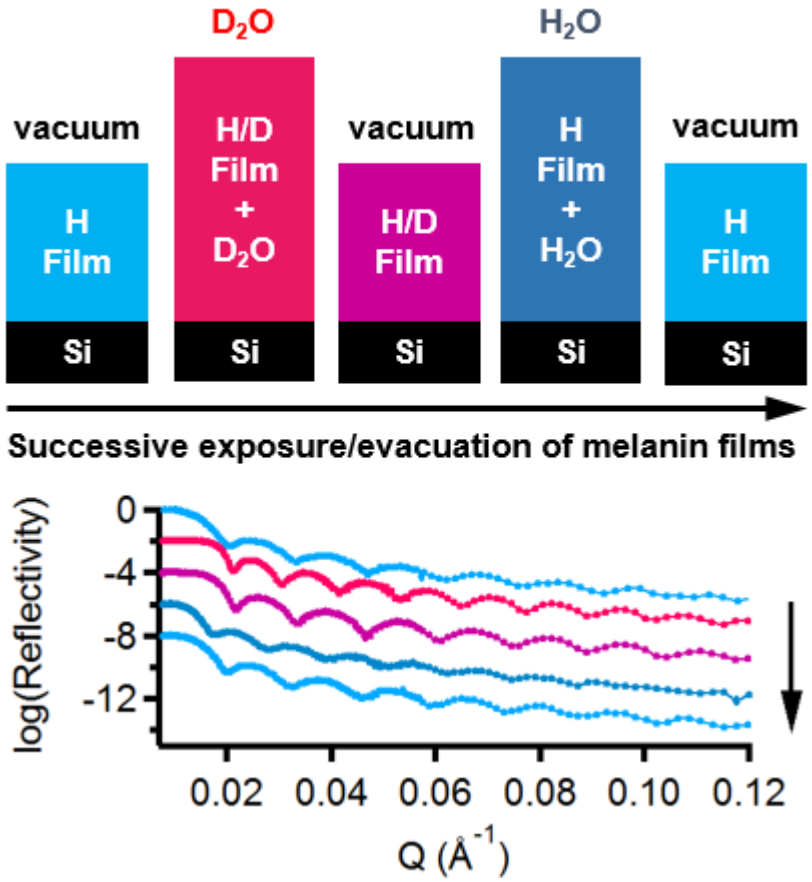
D2O
H2O
vacuum
H/D Film + D2O
vacuum
H/D Film
vacuum
H Film + H2O
vacuum
H Film
Si
Si
Si
Si
Si
Successive exposure/evacuation of melanin films
log(Reflectivity)
0
-4
-8
-12
0.02
0.04
0.06
0.08
0.10
0.12
Q (Å-1)